A planar catalytic combustion sensor using nano-crystalline F-doped SnO₂ as a supporting material for hydrogen detection

Chi-Hwan Han[†], Dae-Ung Hong, Jihye Gwak and Sang-Do Han

Photo- & Electro-Materials Research Center, Korea Institute of Energy Research,
71-2, Jang-dong, Yuseong, Daejeon 305-343, Korea

Abstract−A planar catalytic combustion gas sensor based on Pd/Pt catalyst supported on F-doped SnO₂ nano-crystalline materials has been designed and fabricated for hydrogen detection. The sensor consists of platinum heaters on an alumina plate coated with a catalytic layer and compensating layer. This sensor exhibited better performance than that of the sensors employing sensing material of Pd/Pt catalyst on γ-Al₂O₃ and of Pd/Pt catalyst on nano-crystalline SnO₂. The detection limit of the sensor at 370 °C is in the concentration range of 0.5-5% (v/v), with an excellent linearity of signal voltage to the hydrogen gas concentration.

Key words: Hydrogen Sensor, Catalytic Combustion, F-doped SnO₂, Pd/Pt Catalyst

INTRODUCTION

Mankind's energy needs have evolved for centuries and continue to evolve today. From wood and animal fat, to coal, to petroleum, to propane, to natural gas, we have used a succession of fuels to heat us, manufacture our goods, and light our lamps. Hydrogen is the latest in the succession of fuels, with many social, economic, and environmental benefits to its credit. While the nineteenth and twentieth centuries were considered to be the centuries of coal and oil, respectively, the twenty-first century will be the century of hydrogen. The technology is now available to begin converting from a petroleum-based economy to a hydrogen-based one. In order to implement successfully a renewable hydrogen economy, the safe production, storage, transport, handling and use of hydrogen is imperative. Like all fuels, hydrogen has inherent hazards and must be handled carefully. The low viscosity and small molecular size of hydrogen give it a greater propensity to leak than other common gaseous fuels. A gaseous hydrogen leakage of 4% (the lower explosive limit; LEL) in air, at normal conditions, may lead to an explosive atmosphere of easy ignition. Hydrogen is odorless, colorless, and tasteless, so most human senses will not help to detect a leak. For these and other reasons, industry often uses hydrogen sensors to help detect hydrogen leaks, which has stimulated considerable efforts towards developing sensitive, reliable, and cost-effective hydrogen sensors for the fast detection of hydrogen leaks [1-6].

The most commonly used hydrogen sensors in industries or research are the semiconductor type and the catalytic combustion type. Research into metal oxide semiconductor (MOS) devices for gas sensing applications is increasing nowadays. The first reports of hydrogen sensitive Pd MOS based transistor in 1975 by Lundström et al. [7,8] sparked enormous interest in this area. The focus of sensor development concerns the investigation into new materials that provide increased sensitivity, selectivity and stability. Among them,

metal oxide semiconductor devices with different materials are studied for hydrogen gas-sensing applications [9-11]. However, numerous efforts are still being directed to developing a high performance H₂ sensor [12-14].

Although semiconductor gas sensors have the advantage of high sensitivity, they have disadvantages in long-term stability. Catalytic combustion type gas sensors have linear gas response and simple structure, but they show low sensitivity to inflammable gases due to the lack of adsorption sites of their catalysts and low temperature coefficient of the heater resistance [15]. Other serious problems of catalytic type gas sensors are heat loss (power loss) and poisoning. In order to minimize power loss, low thermal conductivity material and thermally isolated device structures should be used. Poisoning occurs when there is strong adsorption of vapors, phosphate esters and sulfur containing compounds. Poisoning induces the loss of sensitivity because the strongly adsorbed gases pre-occupy catalyst sites and inhibit catalytic reaction between catalyst and the detecting gases [16]. In order to overcome disadvantages, it would be a good method for gas sensors to have a combination of catalysts and semiconductor materials. Metal additives such as platinum (Pt), gold (Au) or palladium (Pd) are catalysts that promote chemical reactions by reducing the activation energy between the films and the test gas resulting in high sensitivity and guaranteed stability [17,18]. Porous catalyst Pt/Pd dispersed on γ-alumina has been used to improve the poison resistance of the sensors [19,20]. The metals are used to increase the selectivity and the sensitivity of the sensor as well as reducing the response and recovery times [21]. Moreover, at higher operating temperatures (>100 °C), the H₂ sensitivity is often reported to be higher for the sensor with the Pt-catalyst than without the Pt-catalyst [22].

Recently, the authors have reported on the synthesis of nano-crystalline F-doped SnO₂ and its application to a micro gas sensor [6]. This micro gas sensor has shown higher sensitivity and better selectivity for hydrogen gas in comparison to commercially available SnO₂ sensors because of the greater adsorption of hydrogen molecules on the favorable sites at fluorine atoms of the materials or the increased

[†]To whom correspondence should be addressed.
E-mail: hanchi@kier.re.kr

n-type property of SnO_2 by fluorine doping.

In this study, we fabricated a catalytic combustion type hydrogen sensor with a good sensitivity, long-term stability and simple structure using Pd/Pt catalysts supported on F-doped SnO_2 materials. The fabricated device exhibits the advantages of high hydrogen detection sensitivity and linearity to high concentration of hydrogen.

EXPERIMENTAL

1. Synthesis and Characterization of the F-doped SnO_2 Material

The sol-gel precursor fluoro(2-methylbutan-2-oxy)di(pentan-2,4-dionato)tin(II) was prepared by the procedure described elsewhere [6]. Solvents used were dried over calcium hydride (acetonitrile) or sodium/benzophenone (pentane) and distilled. A mixture of water (6.8 g, 378 mmol) and acetonitrile (18.2 mL) was added dropwise to a stirred solution of fluoro(2-methylbutan-2-oxy)di(pentan-2,4-dionato)tin (16.01 g, 37.8 mmol) in acetonitrile (80 mL). After the mixture was stirred for 20 min, sol-gel transition occurred and the resulting gel was aged at room temperature for two days. Volatiles were then removed under reduced pressure at 70 °C to give white powders, which were then washed three times with 80 ml of n-pentane. After drying under vacuum at 80 °C, 7.4 g of a yellowish powder was obtained. Elemental analysis: calculated for $SnF_{0.8}(OH)_{0.8}$ $O_{1.1}(C_5H_7O_2)_{0.2}0.8H_2O$; wt% Sn=59.5, wt% C=6.0, wt% F=7.6, wt% H_2O=7.2; found : wt% Sn=58.8, wt% C=5.8, wt% F=7.6, wt% H_2O=7.4. Calcinations were performed by treating the yellowish powder in air for 30 min at a temperature between 400 °C and 550 °C. The chemical composition of the resulting powders was determined by microanalysis: powder calcined at 550 °C; (expt.) wt% Sn=73.7, wt% C=0.25, wt% F=0.25. The synthesized F-doped SnO_2 material was characterized by XRD, SEM and TEM. Crystallinity of the materials was evaluated by powder X-ray diffraction by using a Philips PW 1280 diffractometer. Particle size and morphology of the samples were observed by SEM and TEM using Philips XL30 and JEOL-JEM 100SX microscope models, respectively.

2. Fabrication of the Planar Catalytic Combustion Sensor

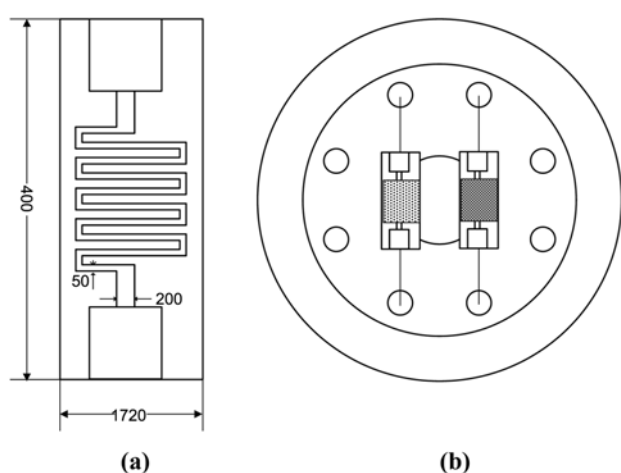Fig. 1 schematically shows the structure and size of the present sensor device. The sensor device was fabricated by the following procedure. A platinum micro-heater was formed on an alumina plate by a screen-printing method with platinum paste (METECH, Platinum conductor PCC 11417) and heat treatment at 1,000 °C for 10 min. The sensing element was formed by drop coating of a catalytic layer on the platinum heater, followed by firing at 700 °C for 1 h in a muffle furnace. The compensating element was also formed by the same method with an inert layer. Then, the sensing and compensating elements were linked to signal pins of the sensor body by a spot welder (WITH Corporation, WMH-V1) with platinum wire (thickness: 30 mm). The compensating element formed one arm of the Wheatstone bridge. The sensor element was connected in series with the bridge, such that nearly the same current flowed through the compensating element and the sensor element. The surface temperature of the sensor at each applied voltage was measured by an IR radiation thermometer (Minolta IR 0506C).

The sensing material as a combustion catalyst for hydrogen was Pd/Pt supported on nano size F-doped SnO_2 at an amount of 15 wt%, and the reference material to compensate the heat capacity of it in a bridge circuit was an inactive γ-Al_2O_3 film. For comparison, sensors coated with a sensing material of Pd/Pt catalyst supported on γ-Al_2O_3 and of Pd/Pt catalyst supported on nano-crystalline SnO_2 was also fabricated. Commercially available nano size SnO_2 (~18.3 nm) and γ-Al_2O_3 (40-47 nm) was purchased from the Aldrich Co. The catalyst layers were deposited with a viscous paste, which was a mixture of oxide powders and organic vehicle. The metal oxide powder material was mixed with an organic vehicle at a concentration of 20 wt% followed by ball-milling for 24 h, to prepare the pastes suitable for screen-printing. The organic vehicle was prepared by dissolving 10 g polyvinyl alcohol resin in a mixed solution of 13 mmol n-butyl alcohol and 350 mmol α-terpineol followed by vigorous stirring at 80 °C.

3. Gas Sensitivity Measurement

All sensing experiments were carried out by using an environmental test chamber, a schematic view of which is shown in Fig. 2. Fresh air was let in and then the gas inlets and outlets of the chamber were closed. The device was exposed to hydrogen gas sample for ~5 s for gas response test and the device was recovered by ex-
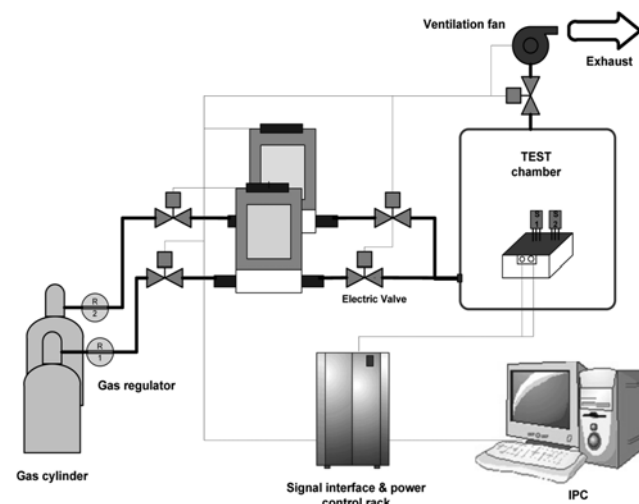

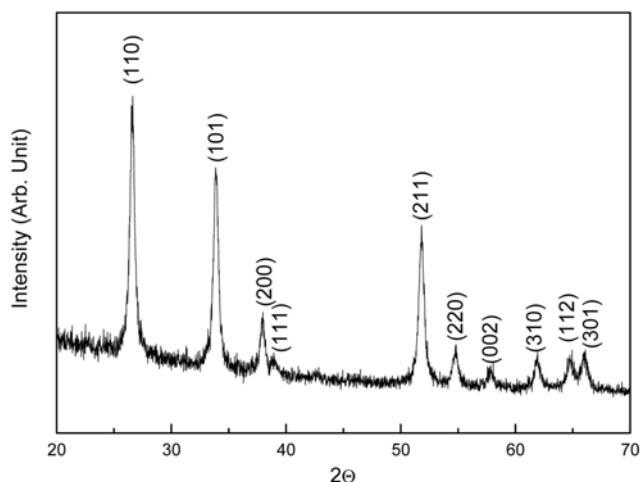Fig. 1. Schematic diagrams of (a) the sensor structure and (b) the fabricated sensor (Dimensions in mm).

Fig. 2. Schematic view of the measuring system.

Fig. 3. XRD pattern of F-doped SnO$_2$ calcined at 550 °C for 30 min.

(a)

(b)

Fig. 4. Micrographs of F-doped SnO$_2$ (a) SEM and (b) TEM.

posure to purified air. Hydrogen and air from commercial gas cylinders were used in most of the experiments. The controller output voltages were measured as the chamber reached the desirable conditions. Sensor response ΔV was defined as the difference between the output voltage in a sample gas (V_g) and that in air (V_a): $\Delta V= V_g - V_a$. The sensing results obtained with the sensor employing Pd/Pt catalyst on F-doped nano-crystalline SnO$_2$ were compared with those of the sensors employing sensing materials of Pd/Pt catalyst on γ-Al$_2$O$_3$ and of Pd/Pt catalyst on nano-crystalline SnO$_2$.

RESULTS AND DISCUSSION

1. Nano-crystalline Sensor Material

XRD pattern of F-doped SnO$_2$ sample is shown in Fig. 3. The F-doped SnO$_2$ had a cassiterite structure without any impurity when calcined at 550 °C for 30 min. All the peaks of the sample can be indexed well to the perfect single-phase material, which is in excellent agreement with the reference pattern (JCPDS 41-1445). However, calcinations at lower temperatures could not produce a well-defined crystalline material. The size of the crystallites can be estimated with the help of the Scherrer equation, $D=0.941\lambda/\beta\cos\theta$, where D is the average crystallite size, λ the X-ray wavelength (0.15405 nm), and θ and β are the diffraction angle and full-width at half-maximum (FWHM, in radian) of an observed peak, respectively [23]. The calculated average crystal size (D) of nano-crystals was found to be 26 nm. The surface morphological features of the nano-crystals were studied by Philips XL30, scanning electron microscope (SEM). The micrograph as shown in Fig. 4(a) reveals that the crystals exhibit narrow size distribution with a slight agglomerate phenomenon. The size of the crystals is in the range of 26-28 nm, which is in favor of a uniform distribution and presence of nano- sized crystals of F-doped SnO$_2$. The TEM image of the F-doped SnO$_2$ sample is shown in Fig. 4(b). It was observed that the material prepared at 80 °C had sponge topology with numerous small pores and the size was 2-5 nm. After calcinations the network aggregated and the size increased to 24-30 nm at 550 °C, consequently reducing the surface area. The BET surface area of material prepared at 550 °C was found to be 70 m^2/g, in comparison to 8.9 m^2/g for the commercial SnO$_2$ (particle size ~10 μm). The resistivity determined at room temperature
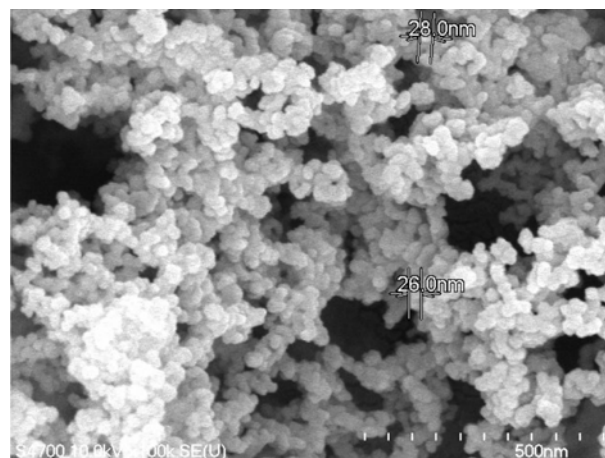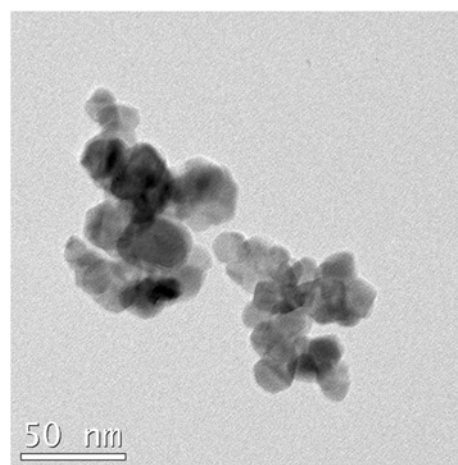
was 1.8 Ω cm for the F-doped SnO$_2$ material made at 550 °C, while commercial SnO$_2$ had a value of 91.3 Ω cm. Low resistivity of the sample is clearly due to the fluorine doping, increasing thereby the n-type character of the SnO$_2$.

2. Temperature of the Sensor

Changes in heater resistance were monitored when a linearly increasing current was applied to the heaters. The resistance was converted to sensor temperature according to the well-known equation [24]:

$$R_{T2}=R_{T1}[1+\alpha(T_2-T_1)]$$

where R_{T1} is the resistance at the initial temperature, R_{T2} is the resistance at the final temperature, α is the temperature coefficient (+0.00377/°C), T_1 is the initial temperature, and T_2 is the final temperature.

The calculated temperature of the heater was compared with the measured temperature by IR gun. Fig. 5 shows the measured and calculated temperatures with the increase in heater voltage. Measured temperature and calculated temperature were well fitted as indicated.
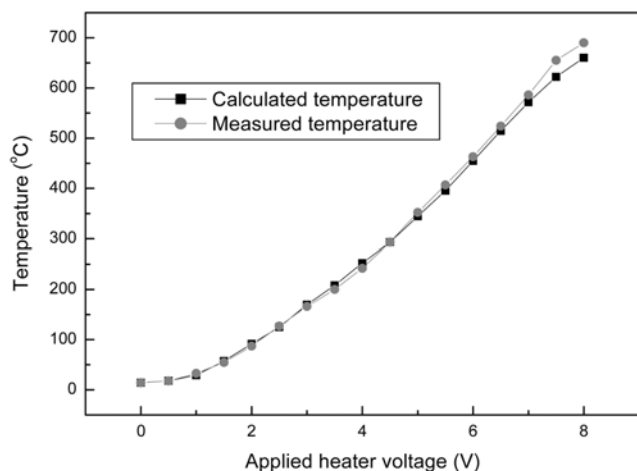
3. Sensing Properties

Fig. 5. Measured and calculated temperature vs. heater voltage.

The lowest limit of hydrogen concentration in air to explosion is 4.65% by volume ratio of hydrogen to air [25]. The range of flammability of hydrogen in air is 4% to 75% by volume. In many accidental situations the lower flammable limit (LFL) is more important. So, a sensor with high performance should be to detect from ppm level to a small percentage of the gas in air. In this study, the detection of 0.5-5% (v/v) concentration range of hydrogen was kept as a target. The sensing activity was tested by keeping the test chamber at room temperature; however, all these measurements were carried out by maintaining the heater temperature between 50 °C and 400 °C. The controller output voltages were measured as the chamber reached the desirable conditions. Sensor response ΔV was defined as the difference between the output voltage in a sample gas (V_g) and that in air (V_a): $\Delta V = V_g - V_a$. The sensing results obtained with the sensor employing Pd/Pt catalyst on F-doped nano-crystalline SnO_2 were compared with those of the sensors employing sensing material of Pd/Pt catalyst on γ-Al_2O_3 and of Pd/Pt catalyst on nano-crystalline SnO_2.

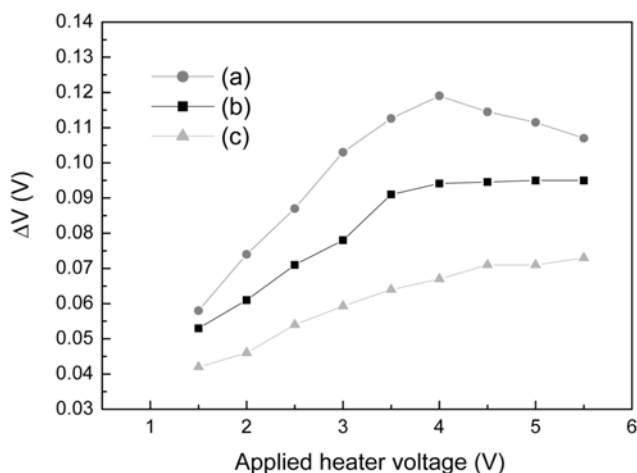For investigation of sensor performance, hydrogen gas and air were mixed in the desired ratio and allowed to flow through the test chamber. A mass flow controller (MFC) was employed to fix the hydrogen flow rate. The concentration of hydrogen was controlled by selecting appropriate values of the flow rates [16]. In the absence of hydrogen gas, temperatures of sensor element and compensation element remain the same and no change in resistance and voltage takes place. On exposure to air containing H_2, there is an increase in the temperature of the active element, resulting in a voltage difference between the compensating element and sensor element. As shown in Fig. 6, this change in voltage was exploited for sensing properties of the different sensors. It is clear from Fig. 6 that sensing performance of the sensor using Pd/Pt catalyst on F-doped nano-crystalline SnO_2 was better than that of the sensors employing sensing material of Pd/Pt catalyst on γ-Al_2O_3 and of Pd/Pt catalyst on nano-crystalline SnO_2. This may be due to the fast catalytic reaction at the surface of F-doped nano-crystalline SnO_2.

The higher response of the nano-crystalline F-doped SnO_2 for hydrogen gas may be due to the greater adsorption of hydrogen molecules on the favorable sites at fluorine atoms of the materials or the increased n-type property of SnO_2 by fluorine doping. It seems the adsorption of hydrogen species is enhanced on the F-doped SnO_2. This causes hydrogen species to become activated and react readily, resulting in a fast catalytic reaction. In the field of catalytic gas sensors, it is well known that an oxidation reaction takes place only on the Pd/Pt catalyst surface and a higher temperature (≥ 200 °C) is required for the maximum sensor response. Thus the Pd/Pt surface promotes catalytic dissociation of hydrogen molecules, and the hydrogen atoms formed are adsorbed on the F-doped SnO_2 surface and then react with already adsorbed and activated oxygen species.

Fig. 7 shows a relationship between the change of voltage and the hydrogen concentration at 4 V of applied heater voltage. It was observed that the voltage difference was proportional to the hydrogen in the concentration range 0.5-5% (v/v). Sensing response of this sensor was found to be high at 4 V in all the cases. As the amount of heat and the resulting voltage were directly related to the existence of hydrogen in air and its concentration, a monitor or concentration measurement system in ambient atmosphere for the safety use of hydrogen could be realized.
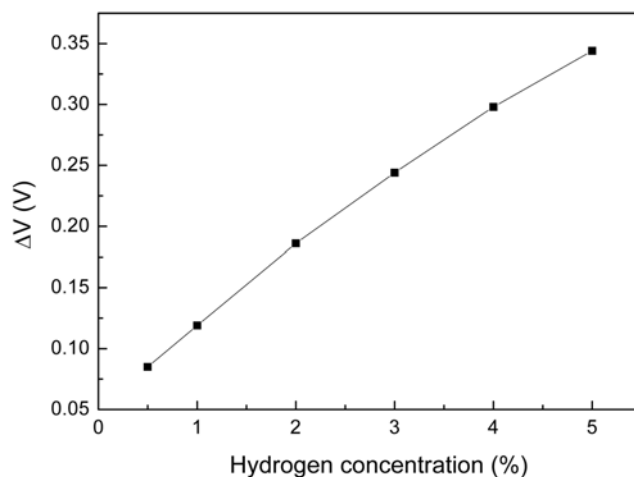

Fig. 6. Response of sensors prepared with different materials of (a) Pd/Pt+F-doped SnO_2, (b) Pd/Pt+γ-Al_2O_3, and (c) Pd/Pt+ SnO_2.

Fig. 7. Relationship between sensitivity and hydrogen concentration at 4 V of applied heater voltage.

CONCLUSIONS

We have reported Pd/Pt supported on nano-size F-doped SnO_2, planar catalytic type sensors that have been fabricated for H_2 concentration measurement in the range of 0-5% (v/v). A simple circuit for operation of the sensors has been described. The maximum hydrogen sensitivity of the sensor is at an operation temperature of 370 °C. Sensing results obtained with the sensor reveal that the sensors based on Pd/Pt catalyst supported on F-doped SnO_2 nano-crystalline system exhibited better performance than Pd/Pt catalyst on γ-Al_2O_3 and than Pd/Pt catalyst on nano-crystalline SnO_2. The higher response of the nano-crystalline F-doped SnO_2 for hydrogen gas may be due to the enhanced adsorption of hydrogen molecules on the favorable sites at fluorine atoms of the materials.

ACKNOWLEDGMENTS

REFERENCES

1. C.-H. Han, S.-D. Han and I. Singh, *Korean J. Chem. Eng.*, **23**, 362 (2006).
2. W. Shin, K. Imai, N. Izu and N. Murayama, *Japanese J. Appl. Phys.*, **40**, 1232 (2001).
3. X. Bevenot, A. Trouillet, C. Veillas, H. Gagnarie and M. Clement, *Sensors & Actuators, B*, **67**, 57 (2000).
4. M. Matsumiya, W. Shin, N. Izu and N. Murayama, *Sensors & Actuators, B*, **93**, 309 (2003).
5. K. Tajima, F. Qiu, W. Shin, N. Sawaguchi, N. Izu, I. Matsubara and N. Murayama, *Japanese J. Appl. Phys.*, **43**, 5978 (2004).
6. C.-H. Han, S.-D. Han, I. Singh and T. Toupance, *Sensors & Actuators, B*, **109**, 264 (2005).
7. I. Lundström, S. Shivaraman, C. Svensson and L. Lundkvist, *Appl. Phys. Lett.*, **26**, 55 (1975).
8. I. Lundström, M. S. Shivaraman and C. M. Svensson, *J. Appl. Phys.*, **46**, 3876 (1975).
9. A. Trinchi, S. Kaciulis, L. Pandolfi, M. K. Ghantasala, Y. Y. Li, W. Wlodarski, S. Viticoli, E. Comini and G. Sberveglieri, *Sensors & Actuators, B*, **103**, 129 (2004).
10. B. S. Kang, S. Kim, F. Ren, B. P. Gila, C. R. Abernathy and S. J. Pearton, *Sensors & Actuators, B*, **104**, 232 (2005).
11. C.-T. Lu, K.-W. Lin, H.-I. Chen, H.-M. Chuang, C.-Y. Chen and W.-C. Liu, *IEEE Electron Dev. Lett.*, **24**, 390 (2002).
12. K. Katahira, H. Matsumoto, H. Iwahara, K. Koide and T. Iwamoto, *Sensors & Actuators, B*, **73**, 130 (2001).
13. T. Hyodo, S. Abe, Y. Shimizu and M. Egashira, *Sensors & Actuators, B*, **93**, 590 (2003).
14. U.-S. Choi, G. Sakai, K. Shimanoe and N. Yamazoe, *Sensors & Actuators, B*, **98**, 166 (2004).
15. M. G. Jones and T. G. Nevell, *Sensors & Actuators*, **16**, 215 (1989).
16. V. R. Katti, A. K. Dehnath, S. C. Gadkari, S. K. Gupta and V. C. Sahni, *Sensors & Actuators, B*, **84**, 219 (2002).
17. A. Cabot, A. Vila and J. R. Morante, *Sensors & Actuators, B*, **84**, 12 (2002).
18. P. Montmeat, C. Pijolat, G. Tournier and J.-P. Viricelle, *Sensors & Actuators, B*, **84**, 148 (2002).
19. D. W. Dabill, S. J. Gentry and P. T. Walsh, *Sensors & Actuators*, **11**, 135 (1987).
20. S. J. Gentry and P. T. Walsh, *Sensors & Actuators*, **5**, 239 (1984).
21. J. Mizsei, P. Sipila and V. Lantto, *Sensors & Actuators, B*, **47**, 139 (1998).
22. A. Dieguez, A. Vila, A. Cabot, A. R. Rodriguez, J. R. Morante, J. Kappler, N. Barsan, U. Weimar and W. Gopel, *Sensors & Actuators, B*, **68**, 94 (2000).
23. J. M. Nedelec, D. Avignant and R. Mahiou, *Chemistry Materials*, **14**, 651 (2002).
24. J. J. Carr, *Sensors and circuits*, PTR Prentice Hall, Englewood Cliffs, New Jersey, US, 07632, p. 75 (1993).
25. R. C. Weast, *Handbook of chemistry and physics*, CRC Press, Cleveland, US, p. D-107 (1976).